CHEMICAL ENGINEERING TRANSACTIONS
VOL. 86, 2021
A publication of AIDIC
The Italian Association of Chemical Engineering
Online at www.cetjournal.it
Guest Editors: Sauro Pierucci, Jiří Jaromír Klemeš

ISBN 978-88-95608-84-6; **ISSN** 2283-9216

Numerical Modelling of Steam Reforming of Methane (SRM) in a Thermochemical Packed Bed Reformer on the Open-Cell Foams: A Computer Simulation

Daniel Ribeiro Dessaune [a], Jornandes Dias da Silva[a,*]

Polytechnic School - UPE, Laboratory of Environmental and Energetic Technology; Rua Benfica - 455, Madalena, Recife - PE, Brazil, Cep: 50750-470
jornandesdias@poli.br

The hydrodynamic characterization of the Steam Reforming of Methane (SRM) through β-SiC open-cell foam in packed bed configuration is performed by reacting Methane (CH_4) with water steam (H_2O). The physical-mathematical modelling is important to design and optimize the SRM method. Usually, the SRM method's application through β-SiC foam bed improves the heat transfer and mass transfer due to high porosity and surface area of the β-SiC foam. This work has as main objective a theoretical modelling to describe the process variables of the SRM method in the TPB reformer. The TPB reformer is filled with β-SiC open-cell foam where the thermochemical conversion of CH_4 is carried out. The model variables describe the specific aims of work and these objectives can be identified from each equation of the developed mathematical model. This work has been proposed to study two specific aims as (i) The effective thermal conductivity's effect of the solid phase ($\lambda_{s,eff.}$) and (ii) molar flows of chemical components. The endothermic reaction temperature's profiles are notably increased as the numeral value of $\lambda_{s,eff.}$ is rised. The SRM method is suggested to improve the Production Rate (PR) of H_2 regarding the PR of CO. As results, the PR of H_2 is of 29.48% while the PR of CO is of 2.76%.

1. Introduction

The production of hydrogen (H_2) can be carried out from different methods such as thermochemical method (heat and chemical reactions to produce H_2), Reforming of hydrocarbons, electrolytic method (Lima et al., 2020) biomass gasification, coal gasification, and biological method (Anjos et al., 2020). The production of H_2 in packed bed reformers is still attracting the interest of researchers and engineers. Up to date, several works have been published in the literature dealing with reforming method to produce H_2 on different commercial catalyst (Yu et al., 2017). This work has as novelty the thermochemical conversion of CH_4 on a β-SiC open-cell foam in a Thermochemical Packed Bed (TPB) reformer. β-SiC open-cell foams have been considered as potential candidates for catalyst support in the heterogeneous catalysis field due to their high external surface area combined with a low pressure drop (Chen et al., 2018). On the other hand, foam-based packed bed reformers offer great potential advantages for the thermal energy storage due to bed's high porosity.
The hydrodynamic characterization of the Steam Reforming of Methane (SRM) through β-SiC open-cell foam in a packed bed configuration in the TPB reformer is performed by reacting Methane (CH_4) with water steam (H_2O). A physical-mathematical modelling is important to design and optimize the SRM method in the TPB reformer. Usually, the SRM method's application through β-SiC foam bed improves the heat transfer and mass transfer due to high porosity and surface area of the β-SiC foam (Vanhaecke et al., 2012). Mass, energy and momentum balance's equations for the gas phase as well as mass, energy and momentum balance's equations to the solid phase are described through mathematical models (Ma et al., 2016). Here, a Non-isothermal Pseudo-Homogeneous mathematical (NIPHM) model is used to model the SRM method in the TPB reformer. The NIPHM model is described by a system of Nonlinear Partial Differential Equations (NPDEs) in together with a developed kinetic model for reforming reactions.

The approach and solution of physical-mathematical models are still a novelty of TPB reformers and thus the topic is a very actual in accessible literature. The novelty of this work lies in the application of open-cell foam (β-SiC) bed for the SRM method. A numerical analysis has been driven to investigate the molar flows of chemical components i on the SRM method of the TPB reformer. In addition, the profiles of the endothermic reaction temperature were also analyzed for the SRM method in the TPB reformer.

2. physical setup

A schematic setup is used to study the thermochemical conversion of the SRM method in TPB reformer according to Fig. 1. The physical model from TPB reformer is shown in Fig. 1 below.

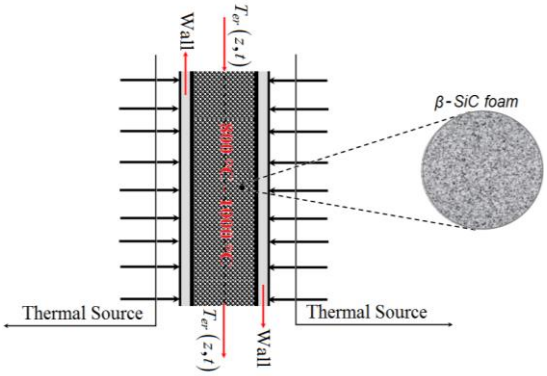

Figure 1: Schematic setup of the physical model from TPB reformer to study the SRM on the β-SiC foam

2.1 Thermochemical kinetic model

The reforming reaction of CH_4 is used to produce syngas (H_2 e CO) and it is highly endothermic (Cruz and Silva, 2017). The SRM process has a limited equilibrium and can be described by the following reforming reaction:

$$SRM: CH_{4(g)} + H_2O_{(g)} \leftrightarrow CO_{(g)} + 3H_{2(g)}\,;\ \Delta H^{0}_{298K} = 205{,}8\,kJ\,/\,mol \tag{1}$$

$$\mathrm{WGSR: CO_{(g)} + H_2O_{(g)} \leftrightarrow CO_{2(g)} + H_{2(g)}\,;\ \Delta H^{0}_{298K} = -41{,}1\,kJ\,/\,mol} \tag{2}$$

The reforming reactions, Eqs. (1) and (2), are based on the Langmuir-Hinshelwood kinetic model (Cruz and Silva, 2017) and its kinetic rates are reported as:

$$R_{SRM} = \frac{\frac{k_{SRM}}{P_{H_2}^{2.5}}\left(P_{CH_4}\,P_{H_2O} - \frac{P_{H_2}^{3}P_{CO}}{K_{SRM}}\right)}{\left(1 + \frac{F_{H_2O,0}}{F_{CH_4,0}} + \frac{F_{H_2,0}}{F_{CH_4,0}} + K_{CO}P_{CO} + K_{H_2}P_{H_2} + K_{CH_4}P_{CH_4} + \frac{K_{H_2O}P_{H_2O}}{P_{H_2}}\right)^2} \tag{3}$$

$$R_{WGSR} = \frac{\frac{k_{WGSR}}{P_{H_2}}\left(P_{CO}\,P_{H_2O} - \frac{P_{H_2}P_{CO_2}}{K_{WGSR}}\right)}{\left(1 + \frac{F_{H_2O,0}}{F_{CH_4,0}} + \frac{F_{H_2,0}}{F_{CH_4,0}} + K_{CO}P_{CO} + K_{H_2}P_{H_2} + K_{CH_4}P_{CH_4} + \frac{K_{H_2O}P_{H_2O}}{P_{H_2}}\right)^2} \tag{4}$$

3. TPB reformer's mathematical modelling

The development of the NIPHM model takes into account the following assumptions: (1) the NIPHM model is described under non-isothermal condition, (2) the NIPHM model from TPB reformer is plug-flow with axial dispersion under transient condition, (3) the radial dispersion is negligible inside TPB reformer, (4) the

gaseous mixture has constant density in TPB reformer, (5) the molar flow rates inside TPB reformer are constant, (6) the deposition effect of carbon at the surface of catalytic particles has been neglected, (7) the gas behavior inside TPB reformer was considered as an ideal gas mixture, (8) the bed porosity in axial direction is considered constant, (9) the heaviest hydrocarbons than methane haven't been considered in this work, and (10) chemical reactions as assumed to take place at the surface of catalyst particles. These premises are used to build the governing equations of the NIPHD model inside TPB reformer as follows.

3.1 Gas phase's energy balance

A proposed equation provides clear information to drive the temperature distribution on the gas phase under open-cell foam (β-SiC) bed and can be described as follows.

$$\rho_{g,mix.} C_{p,g,mix.} \left(\frac{\partial T_g}{\partial t} + \frac{4 q_g}{\pi d_{refor.}^2} \frac{\partial T_g}{\partial z} \right) = \lambda_{g,eff} \frac{\partial^2 T_g}{\partial z^2} - h_{gs} \frac{\left(1-\varepsilon_b\right)}{\varepsilon_b} \frac{6}{d_p} \left(T_g - T_{er} \right) \tag{7}$$

The suitable initial and boundary conditions from Eq. (7) are given as follows.

$$T_g\Big|_{t=0} = T_{g,0} \; ; \frac{\partial T_g}{\partial z}\bigg|_{z=0^+} = \frac{\rho_{g,mix.} C_{p,g,mix.}}{\lambda_{g,mix.}} \frac{4 q_g}{\pi d_{ref.}^2} \left(T_g\Big|_{z=0^+} - T_{g,\infty} \right); \frac{\partial T_g}{\partial z}\bigg|_{z=L} = 0 \tag{8}$$

3.2 Solid phase's energy balance

The energy balance equation of the solid phase is built at the surface of β-SiC open-cell foams where take place the endothermic reaction of CH_4 and can be reported as follows.

$$\rho_s C_{p,s} \frac{\partial T_{er}}{\partial t} = \lambda_{s,eff} \frac{\partial^2 T_{er}}{\partial z^2} + h_{sg} \frac{6}{d_p} \frac{\left(1-\varepsilon_b\right)}{\varepsilon_b} \left(T_g - T_{er} \right) + \rho_s \frac{\left(1-\varepsilon_p\right)}{\varepsilon_p} \sum_{j=1}^{2} \pm \Delta H_j \, \eta_j R_j \tag{9}$$

The initial and boundary conditions from Eq. (9) are described as:

$$T_{er}\Big|_{t=0} = T_{er,0} \; ; \frac{\partial T_{er}}{\partial z}\bigg|_{z=0^+} = \frac{q_h}{\lambda_s} \; ; \frac{\partial T_{er}}{\partial z}\bigg|_{z=L} = \frac{h_{sg,eff}}{\lambda_{s,eff.}} \left(T_{er,\infty} - T_{er}\Big|_{z=L} \right) \tag{10}$$

3.3 Transport equation of chemical components

In Section 3, it was approached some assumptions that can be used to build the proposed problem's modelling. However, the transport equations for chemical components i (i = CH_4, H_2O, CO, CO and H_2) are presented as follows.

$$\frac{u_{sg}}{g} \frac{\partial F_i}{\partial t} + \frac{4 q_g}{S_{sp} \pi d_{ref.}^2} \frac{\partial F_i}{\partial z} = \frac{D_{ax,i}}{S_{sp}} \frac{\partial^2 F_i}{\partial z^2} + \rho_s \, r_{ref.}^2 \, L \left(1-\varepsilon_b\right) r_i \; ; 0 < z < L \tag{11}$$

The suitable initial and boundary conditions from Eq. (11) are presented as follows.

$$F_i\Big|_{t=0,} = F_{i,0} \; ; \varepsilon_b \frac{D_{ax,i}}{L} \frac{\partial F_i}{\partial z}\bigg|_{z=0^+} = u_{sg} \left(F_i\Big|_{z=0^+} - F_{i,\infty} \right); \frac{D_{ax,i}}{L} \frac{\partial F_i}{\partial z}\bigg|_{z=L} = \frac{k_{gs,eff}}{\varepsilon_b} \left(F_i\Big|_{z=L} - F_{i,\infty} \right) \tag{12}$$

3.4 Numerical solution of the model equation

The CIEA's method can be employed as a good technique for studying the performance from TPB reformers. The CIEA's methodology has been used to transform the PDE system into an ODE system using the boundary conditions of each PDE and can be found in Ref. (Dias and Silva, 2020).

3.5 Results and Discussions

In section 3, a physical-mathematical modelling has been developed to investigate the SRM method in the TPB reformer. A computational algorithm using the FORTRAN 95 has been elaborated by authors to compute the SRM method's variables in the TPB reformer.

3.6 Model parameters

The kinetic and hydrodynamic model's parameters from the TPB reformer were used combined to feed the computational algorithm. The numerical values of these parameters are shown in Table 1 below.

Table 1: Physical parameters used to feed the computer algorithm

parameters	Values	Sources
k_{SRM} (mol (kPa)$^{0.5}$/kg$_{cat.}$ sec.) (1)	2.015 x 10^{11}	Cruz and Silva, 2017
K_{SRM} (kPa)^2 (1)	2.135 x 10^7	Cruz and Silva, 2017
K_{WGSR} (mol (kPa)$^{-1}$/kg$_{cat.}$ sec.)(1)	1.218x10^3	Cruz and Silva, 2017
K_{WGSR} (-)(1)	13.015	Cruz and Silva, 2017
K_{CH4} (kPa)$^{-1}$ (1)	8.974 x 10^{-7}	Cruz and Silva, 2017
K_{H2O} (-)(1)	3.701 x 10^4	Cruz and Silva, 2017
K_{H2} (kPa)$^{-1}$ (1)	8.987x10^{-12}	Cruz and Silva, 2017
K_{CO} (kPa)$^{-1}$ (1)	5.671x10^{-6}	Cruz and Silva, 2017
η_{SRM} (-)(1)	0.021	Cruz and Silva, 2017
η_{WGSR} (-)(1)	0.0169	Cruz and Silva, 2017
L (m)	0.60	Estimated
d_p (m)	3.4 x 10^{-4}	Estimated
$d_{refor.}$ (m)	3.2 x 10^{-3}	Estimated
$T_{g,0}$ (K)	673	Estimated
$T_{er,0}$ (K)	673	Estimated
$P_{op.}$ (kPa)	600	Estimated
$\rho_{g,\ mix.}$ (kg/m^3)	0.1692	Silva and Abreu, 2016
$C_{p,\ g,\ mix.}$ (kJ/kg K)	127.09	Dias and Silva, 2020
q_g (m^3/sec.)	1.201x10^{-6}	Estimated
g (m/sec^2)	9.81	Estimated
S_p (sec^{-1})	3.53 x 10^7	Cruz and Silva, 2017
$\lambda_{g,\ eff}$ (W/m K)	1.078	Dias and Silva, 2020
h_{gs} (W/m^2 K)	1.902	Dias and Silva, 2020
ε_b (m^3 gas/m^3 reformer)	0.39	Dias and Silva, 2020
ε_p (m^3 gas/m^3 reformer)	0.87	Voltolina et al., 2017
$C_{p,\ s}$ (J/kg K)	336.00	Dias and Silva, 2020
$\lambda_{s,\ eff}$ (W/m K)	0.501	Silva and Abreu, 2016
$F_{CH4,0}$ (mol/sec.)	0.25	Silva and Abreu, 2016
$F_{H2O,0}$ (mol/sec.)	0.75	Silva and Abreu, 2016
$F_{H2,0}$ (mol/sec.)	7.62 x 10^{-5}	Silva and Abreu, 2016
$F_{CO,0}$ (mol/sec.)	3.2 x 10^{-5}	Silva and Abreu, 2016
$F_{CO2,0}$ (mol/sec.)	6.32x10^{-5}	Silva and Abreu, 2016
$D_{ax,\ CH4}$ (m^2/sec.)(1)	289 x 10^{-3}	Cruz and Silva, 2017
$D_{ax,\ H2O}$ (m^2/sec.)(1)	3.79 x 10^{-3}	Cruz and Silva, 2017
$D_{ax,\ H2}$ (m^2/sec.)(1)	2.01 x 10^{-3}	Cruz and Silva, 2017
$D_{ax,\ CO}$ (m^2/sec.)(1)	3.41 x 10^{-3}	Cruz and Silva, 2017
$D_{ax,\ CO2}$ (m^2/sec.)(1)	1.89 x 10^{-3}	Cruz and Silva, 2017

(1) Computed at 725°C

3.7 Validation by comparison against published data

To ensure the validity of the proposed model, authors have made a comparison of simulated results with published data of the literature. Slight differences can be found due to the deviation between the literature results and simulating results. An average relative error (ARE), Eq. (12), was used to compute the consistency criterion and therefore, the ARE is given as follows.

$$ARE = \left| \frac{F_i^{Chompupun\ et\ al.,2018} - F_i^{Simulating\ results}}{F_i^{Chompupun\ et\ al.,2018}} \right| x100;\ i = CH_4, H_2O, H_2, CO\ and\ CO_2 \qquad (12)$$

Fig. 2 compares the literature results and simulated results of molar flows of chemical components i at the outlet of the TPB reformer. As it can be seen in Fig. 2, the simulated results against the experimental results

from literature (Chompupun et al., 2018) have presented a good agreement, resulting in AREs of 9.28%, 0.81%, 1.29%, 9.74%, and 2.13%. These AREs should be due to the incompatibility between the simulating results and experimental results.

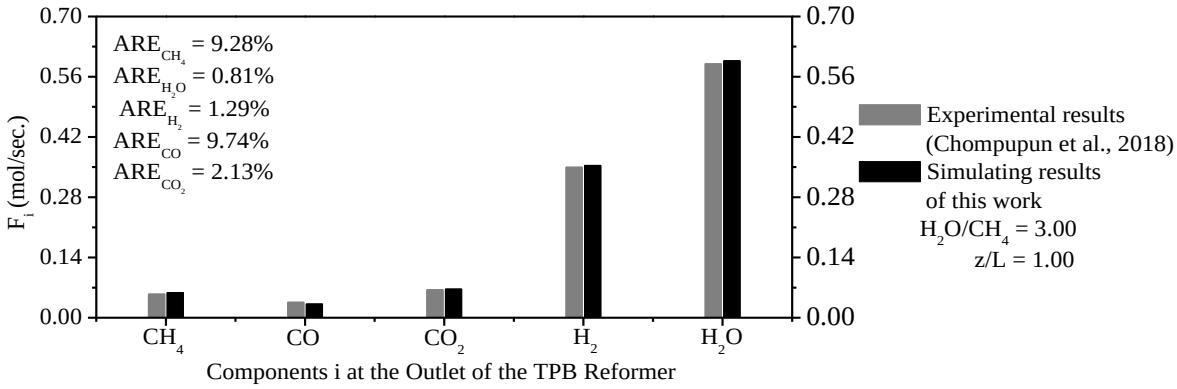

Figure 2: Comparison between molar flows of chemical components i at the outlet of TPB reformer

3.8 Numerical experiments

In Fig. 3, it is checked the dynamic region and stationary region along the TPB reformer's length. The dynamic region occurs up to ± 0.18 m, after that the stationary state is kept until 0.60 m.

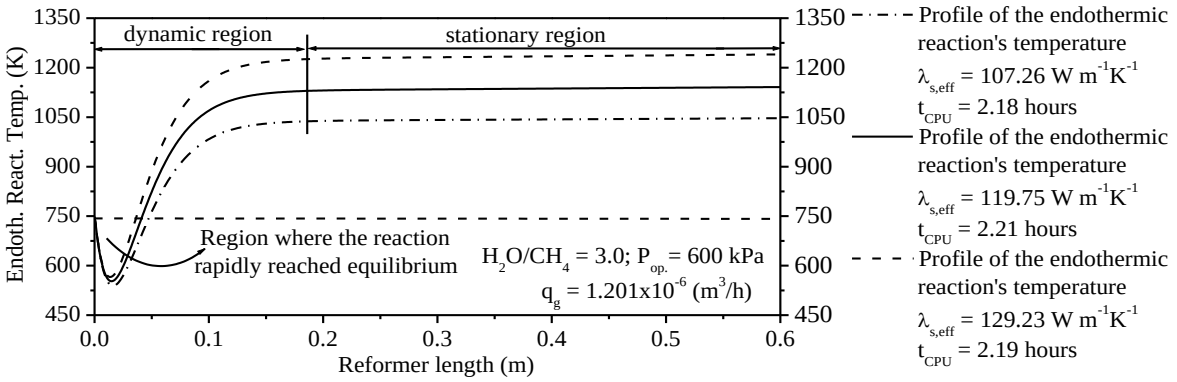

Figure 3: Endothermic reaction temperature's profiles along of the TPB reformer's length on β-SiC foam.

The range of the $\lambda_{s,\,eff.}$ has a pertinent effect on the ERT's profiles in TFB reformer. Three different values of the $\lambda_{s,\,eff.}$ have been used to check the ERT's sensibility to the $\lambda_{s,\,eff.}$. As results, when the $\lambda_{s,\,eff.}$ is higher ($\lambda_{s,\,eff.}$ = 129.23), the heat absorption in TFB reformer is notably increased and therefore, the ERT's profile is favoured. On the other hand, when the $\lambda_{s,\,eff.}$ is lower ($\lambda_{s,\,eff.}$ = 107.26), the heat absorption in TFB reformer is remarkably decreased and thus, the ERT's profile is reduced.

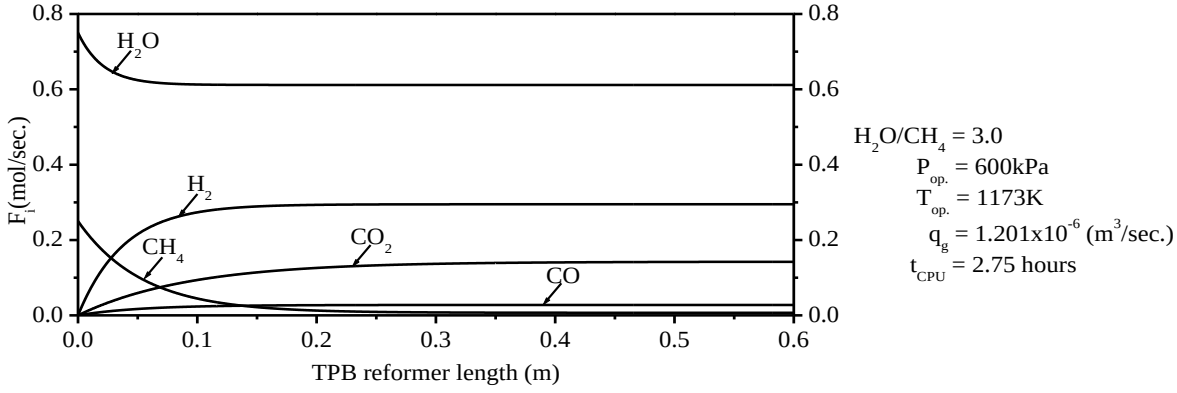

Figure 4: Molar flows of each chemical component i along of the TPB reformer's length on β-SiC foam

Fig. 4 shows the profiles of the molar flow of each chemical component i of the SRM method at the following operating conditions: H_2O/CH_4 = 3.00, 500 kPa, 1173 K, and $1.201x10^{-6}$ (m^3/sec.). In Fig 4, the profiles of the molar flows from the consumed reactants (H_2O and CH_4) and produced products (CO, CO_2 and H_2) are reported in the TPB reformer. After reaching the stable state, only 18.67% of H_2O was consumed. On the other hand, after achieving the stable state, 97.26% of CH_4 was consumed. After reaching the stable state, 29.48% of H_2, 14.23% of CO_2, and 2.76% of CO were produced for the SRM method in the TPB reformer.

4. Conclusions

A non-isothermal pseudo-homogeneous mathematical model which includes the thermal energy transfer on the endothermic thermochemical conversion and mass transfer coupled with a thermochemical kinetic model was developed and validated against published data of the literature for a TPB reformer. After validating the numerical model, such model can be used like a process simulator. Therefore, the major conclusions are listed as follows.

1. The simulating results of molar flows are similar to experimental results of molar flows under same operating conditions. The validating results have driven a good agreement against the literature data for molar flows at the outlet from TPB.
2. When the $\lambda_{s,\ eff.}$ is notably increased, the ERT's profile is rised. On the other hand, when the $\lambda_{s,\ eff.}$ is remarkably reduced, the ERT's profile is decreased.
1. Under the prescribed operating conditions, 18.67% of H_2O and 97.26% of CH_4 were consumed while 29.48% of H_2, 14.23% of CO_2, and 2.76% of CO were produced.

Acknowledgments

The authors of this paper would like to thank CNPq (National Council of Scientific and Technological Development) for the financial support given (Process 48354/2012).

References

Anjos E. B., Silva Filho A. M., Silva J. D., 2020, Numerical simulation of the steam reforming of toluene in a fixed-bed catalytic reformer to produce hydrogen, J Braz. Soc. Mech. Sci. Eng, 42, 114.

Chen, X., Fuqiang, W., Han, Y., Yu, R., Cheng, Z., 2018, Thermochemical storage analysis of the dry reforming of methane in foam solar reactor, Energy Conversion and Management, 158, 489-498.

Chompupun, T., Limtrakul, S., Vatanatham, T., Kanhari, C., Ramachandran, P. A., 2018, Experiments, modeling and scaling-up of membrane reformers for hydrogen production via steam methane reforming, Chemical Engineering Processing, 134, 124-140.

Cruz, B. M., Silva, J. D., 2017, A two-dimensional mathematical model for the catalytic steam reforming of methane in both conventional fixed-bed and fixed-bed membrane reformers for the production of hydrogen, International Journal of Hydrogen Energy, 42, 23670-23690.

Dias, V. F., Silva, J. D., 2020, Mathematical modelling of the solar - driven steam reforming of methanol for a solar thermochemical micro-fluidized bed reformer: thermal performance and thermochemical conversion, Braz. Soc. Mech. Sci Eng., 42, 447.

Ma, Y., He, L., Li, S., Teng, J., 2016, Heat transfer of oil shale in a small-scale fixed bed, Journal of Thermal Analysis and Calorimetry, 124, 461-469.

Lima, K. P. M., Dias, V. F. and Silva, J. D., 2020, Numerical modelling for the solar driven bi-reforming of methane for the production of syngas in a solar thermochemical micro-packed bed reformer, International Journal of Hydrogen Energy, 45, 10353-10369.

Silva, J. D. and Abreu, C. A. M., 2016, Modelling and simulation in conventional fixed-bed and fixed-bed membrane reformers for the steam reforming of methane, International Journal of Hydrogen Energy, 41, 11669-11674.

Vanhaecke, C., Pham-Huu, C., Edouard, D., 2012, Simulation and experimental measurement of dynamic behavior of solid foam filter for diesel exhaust gas, Catalysis Today, 189, 101-110.

Voltolina, S., Marín, P., Díz, F. V., Salvador, O., 2017, Open-cell foams as beds in multiphase reactors: Residence time distribution and mass transfer, Chemical Engineering Journal, 316, 323 – 331.

Yu, T., Yuan, Q., Lu, J., Ding, J. Lu, Y., 2017, Thermochemical storage performances of methane reforming with carbon dioxide in tubular and semi-cavity reactors heated by a solar dish system, Applied Energy, 185, 1994-2004